Surface roughness and thermal evolution of planetary surfaces

P452 : Computational Physics Term Project Report

Submitted To

Dr. Subhasish Basak
Associate Professor
School of Physical Sciences
NISER Bhubaneshwar

Submitted By

Niti Singh
Integrated M.Sc. Physics (2020-25)
NISER Bhubaneshwar

Under Supervision Of

Dr. Guneshwar Thangjam
Reader-F
School of Earth and Planetary Sciences
NISER Bhubaneshwar

April 28th, 2024

Surface roughness and thermal evolution of planetary surfaces

Abstract

In this report, the surface roughness and topography for a general planetary surface was studied while employing a 1D thermal model using the Crank-Nicolson method to solve the heat equation with flux conservation. The methodology involves numerically simulating surface heat distribution and comparing the results with analytical solutions. Then it is modified as incoming solar flux is calculated without considering atmospheric effects, and surface temperature distribution coupled with thermal emission is simulated. The report discusses the implementation of these methods and presents the results obtained. Through numerical simulations and analytical comparisons, insights into surface heat distribution and thermal emission are studied.

1 Objective

The objective of this project is explore the surface roughness and thermal distribution of the planetary surfaces on a broader prospect. To study the thermal evolution is a vast concept and hence the basic 1D Thermal modeling (KRC approach) will be considered in this project due to time constraints and complexities involved beyond that.

2 Theoretical Background

2.1 Overview

The algorithm in the project simulates planetary surface terrains through a combination of fractal methods and crater distribution. Fractal surfaces are generated using fractional Brownian motion, providing random height information. Crater formation is modeled using various profiles, including normal, central mound, flat-bottomed, and concentric, each defined by specific parameters[Yang et al., 2021]. The algorithm ensures realism by preventing overlap between generated craters. Additionally, shading effects are applied to enhance visual representation, simulating light interaction with terrain features. [Helfenstein and Shepard, 1999]
Then, it also includes a simulation for the diffusion of temperature into the ground over time, considering factors such as surface temperature oscillations and variable thermal properties of the material. It employs the Crank-Nicolson finite difference method, a numerical method for solving partial differential equations, to integrate the heat diffusion equation in time while conserving flux.
The algorithm accounts for boundary conditions, including geothermal heat flux at the bottom boundary and prescribed surface temperature oscillations.

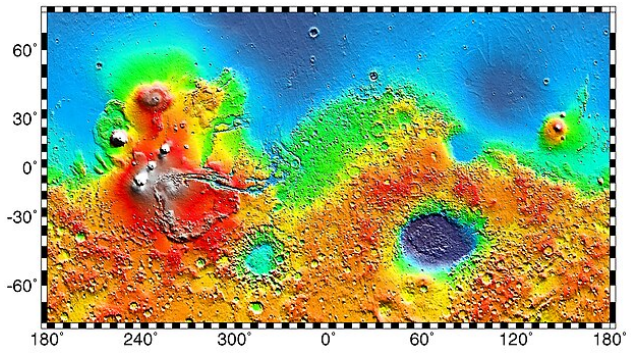

Figure 1: Maps of Mars' global topography. [Credits: NASA/JPL/GSFC]

By discretizing the domain into a grid and iteratively updating the temperature profile, the algorithm captures the evolution of temperature within the ground, providing insights into heat transfer processes and thermal behavior. Then it is modified considering variable thermal properties and irregular grid spacing that accounts for factors such as thermal inertia, geothermal heat flux, and incoming solar radiation. It calculates the temperature profile within the ground over time while ensuring flux conservation and stability through techniques like flux smoothing. By accurately modeling temperature evolution which is to be cross-checked against an analytical solution, the algorithm aids in predicting surface and subsurface temperatures, thermal conductivity variations, and heat flux distributions.

2.2 Fractal Surface Generation

For terrain generation, Fractional Brownian Motion(fBm) is used to model the roughness or irregularity of natural surfaces leveraging its ability to

produce realistic surfaces with fractal characteristics [Bandfield et al., 2015]. It represents a continuous-time stochastic process characterized by its self-similarity and long-range dependence properties where each point's height is influenced by nearby points, with correlations decreasing as distance increases. The parameter r_e controls the roughness or smoothness of the surface. Higher values result in smoother surfaces, while lower values lead to more rugged terrains.

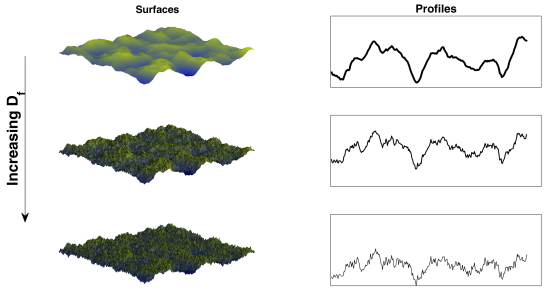

Figure 2: Illustration of surface fractality. Self affine surfaces (left) and surface profiles (right) showing increasing D_f ["Fractal dimension", 2019]

The fractal dimension (D_f) in the figure above is a measure of the complexity or irregularity of a geometric object, such as a terrain surface.

$$D = \lim_{\epsilon \to 0} \frac{\log(N(\epsilon))}{\log(1/\epsilon)}$$

Where: $N(\epsilon)$ is the minimum number of boxes of size ϵ needed to cover the terrain surface and ϵ is the size of the boxes.
This formula provides a way to quantify the self-similarity and irregularity of a terrain surface, where a higher fractal dimension indicates greater complexity and roughness. This process is defined by its covariance function, which determines the statistical correlation between points in the process at different spatial or temporal scales. Mathematically, the covariance function $C(h)$ of fBm can be expressed as:

$$C(h) = \frac{1}{2}\left(|h|^{2H} + |h'|^{2H} - |h - h'|^{2H}\right)$$

Here, H represents the Hurst parameter, a crucial parameter governing the roughness or smoothness of the fBm process. Hence here, $H = r_e$. The covariance function encapsulates the spatial correlation structure of the fBm process, specifying how height values at different points in the terrain are related to each other as a function of their spatial separation h.
The fBm process is discretized to operate on a grid of points representing the terrain surface. The height values for each grid point are generated by sampling from the fBm process, incorporating appropriate scaling factors and adjustments to achieve desired statistical properties. The generated height information is often represented in the frequency domain initially, using Fourier analysis to analyze its frequency content and spatial characteristics.
To convert the height values from the frequency domain to the spatial domain, the **Inverse Fourier transform** is applied by reconstructing the terrain surface from its frequency components, ensuring that it exhibits the fractal-like properties specified by the fBm process.[Shepard et al., 1995] Mathematically, the inverse Fourier transform of a two-dimensional function $Z(u, v)$ is given by:

$$z(x, y) = \text{ifft2}(Z(u, v))$$

$$z(x, y) = \int_{-\infty}^{\infty} \int_{-\infty}^{\infty} Z(u, v) e^{i2\pi(ux+vy)}\, du\, dv \qquad (1)$$

where x and y are spatial coordinates, u and v are frequency coordinates, and i is the imaginary unit. The final terrain surface is a manifestation of the underlying stochastic process, capturing its self-similar and long-range dependence properties.

2.3 Heat Diffusion Equation

The fundamental principle governing the distribution of temperature within a material is encapsulated in the heat diffusion equation. Derived from Fourier's law of heat conduction and the conservation of energy principle, this equation provides a mathematical description of how heat flows through a material over time. In its simplest form, the one-dimensional heat diffusion equation in Cartesian coordinates is expressed as:

$$\rho c \frac{\partial T}{\partial t} = \frac{\partial}{\partial z}\left(k \frac{\partial T}{\partial z}\right)$$

Here, ρ represents the density of the material, c denotes the specific heat capacity, T signifies the temperature, t stands for time, k is the thermal conductivity, and z is the spatial coordinate.
The equation elucidates that the rate of change of temperature ($\frac{\partial T}{\partial t}$) within the material is proportional to the second derivative of temperature with respect to spatial coordinates ($\frac{\partial^2 T}{\partial z^2}$), with the proportionality constant determined by the material's properties[Schorghofer and Aharonson, 2014].

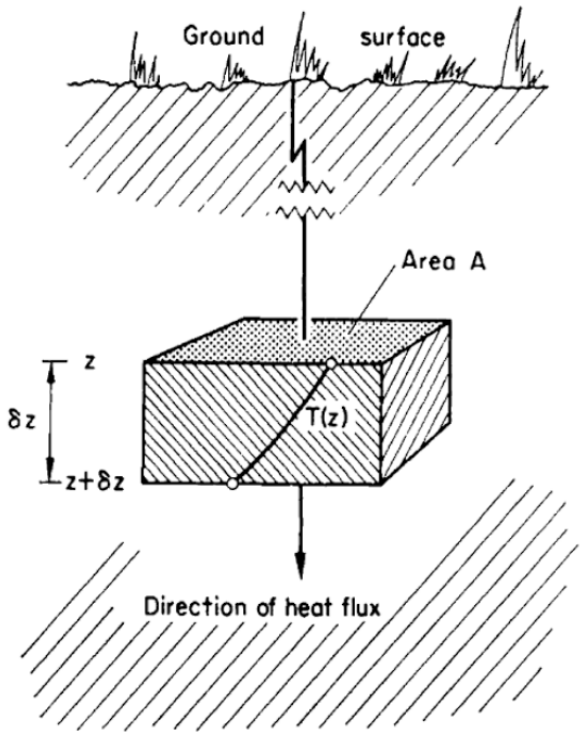

Figure 3: One dimensional heat conduction [Rose, 1966]

$\rho c \frac{\partial T}{\partial t}$ signifies the rate of change of internal energy density with respect to time, reflecting how temperature evolves over time due to thermal processes. $\frac{\partial}{\partial z}\left(k\frac{\partial T}{\partial z}\right)$ captures the flow of heat through the material, with $k\frac{\partial T}{\partial z}$ representing the heat flux. This term elucidates how heat propagates within the material, moving from regions of higher temperature to regions of lower temperature.

2.4 Surface Energy Balance

The surface energy balance equation addresses the energy exchange occurring between the material's surface and its surroundings, incorporating factors such as incoming solar radiation and thermal emission. In its basic formulation, it can be represented as:

$$\Phi(t) = -k\frac{\partial T}{\partial z}$$

Where $\Phi(t)$ denotes the heat flux at the surface boundary, equivalent to the negative of the product of thermal conductivity (k) and the spatial temperature gradient ($\frac{\partial T}{\partial z}$).
This equation can be expanded to include terms accounting for absorbed solar radiation ($Q_a(t)$) and thermal emission ($\varepsilon\sigma T^4$) at the surface:

$$\Phi(t) = -k\left(\frac{\partial T}{\partial z}\right)_0 = Q_a(t) - (\varepsilon\sigma T^4)_0$$

Here, $Q_a(t)$ represents the absorbed solar radiation, ε denotes the emissivity of the surface, σ signifies the Stefan-Boltzmann constant, and T is the temperature. The equation elucidates the equilibrium between incoming and outgoing energy at the material's surface. $-k\frac{\partial T}{\partial z}$ signifies the heat flux into or out of the material at the surface due to conduction. $Q_a(t)$ represents the energy absorbed from incoming solar radiation, while $(\varepsilon\sigma T^4)_0$ denotes the energy emitted from the surface due to thermal radiation, where ε is the surface emissivity and σ is the Stefan-Boltzmann constant.

3 Method

3.1 Topography generation

This code defines a class 'SurfaceModel' that generates a simulated planetary surface based on various parameters. Here's a brief overview of the algorithm pipeline:

- The class is initialized with parameters (based on lunar data [Leahy, 2021] well established by various NASA missions like Apollo, LRO etc) and a seed for random number generation.
- Setting Terrain Environment: If crater generation is enabled ('is_crater'), it generates craters based on specified distribution methods (single or random) and properties. If fractal surface generation is enabled ('$is_fractal$'), it generates a fractal surface using fractional Brownian motion.
- Crater Generation: Various crater models (described in A.1.2) ('normal', 'central mound', 'flat-bottomed', 'concentric') are implemented to generate crater height information based on given parameters and the craters are placed randomly or at specified positions on the terrain.

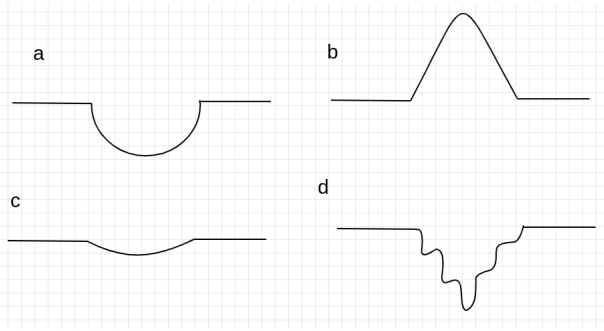

Figure 4: Types of craters (a)Normal; (b)Central mound; (c)Flat; (d) Multi-rim concentric

- Fractal Surface Generation: Utilizes fractional Brownian motion to generate random height information for a fractal surface. Practically, when dealing with discrete data, such as in numerical simulations, the integral in equation given in Eq. 1 is replaced by a discrete sum over the discrete frequencies:

$$z(x,y) = \sum_{u=0}^{N-1} \sum_{v=0}^{M-1} Z(u,v) e^{i2\pi(\frac{ux}{N} + \frac{vy}{M})}$$

  where N and M are the number of samples along the u and v axes, respectively.

- Shading effects: Creates shading effects using color and height information and generates RGB information for terrain appearance, including shading conditions.

Thus, the algorithm generates a synthetic planetary surface with features such as craters and fractal terrain, allowing for customizable parameters and realistic terrain simulations.

3.2 1D Thermal distribution

The code simulates the one-dimensional heat diffusion in a subsurface environment subjected to solar flux variations. The simulation is carried out using two algorithms: Algorithm 1 ('conductionT') and Algorithm 2 ('conductionQ'). The pipeline of the work can be summarized as follows:

- Initialization: Define constants such as the solar constant (`So`), Stefan-Boltzmann constant (`sigSB`), period of oscillation (`Period`), number of time steps (`NSTEPS`), emissivity (`emiss`), albedo (`albedo`), latitude (`latitude`), and parameters related to thermal inertia (`thIn`). Set up the grid for depth (`z`) using either regular or geometric spacing (`setgrid` function). Initialize surface temperature (`T`), mean temperature (`Tmean`), and mean flux (`Fmean`).

- Simulation Loop
  - Iterate over each time step using a `for` loop ranging from 0 to `NSTEPS`.
  - Calculate the hour angle (`HA`) based on the current time and period.
  - Compute the solar flux (`Qn`, `Qnp1`) using the `flux_noatm` function, considering parameters like distance from the sun, solar declination, latitude, hour angle, surface slope, and azimuth of the topographic gradient.
  - Perform the heat diffusion simulation using either Algorithm 1 (`conductionT`) and Algorithm 2 (`conductionQ`).
  - Update the surface temperature, mean temperature, and mean flux based on the results of the simulation and write surface temperature and temperature profile data to output files for further analysis.

- Algorithm 1, referred to as conductionT, employs a Crank-Nicholson finite difference scheme [A.2.1] to solve the heat diffusion equation under flux conservation. This approach accurately models the evolution of temperature profiles while ensuring numerical stability. The algorithm discretizes the subsurface into layers and utilizes grid spacing determined by specified parameters, either regular or geometric. By constructing a tridiagonal matrix representation of the discretized heat equation, Algorithm 1 efficiently solves for temperature distributions across the subsurface domain. It accounts for boundary conditions, including prescribed surface temperature and geothermal heat flux at the bottom boundary, providing a comprehensive simulation of heat transfer processes.

- Algorithm 2, denoted as conductionQ, builds upon the principles of Algorithm 1 but incorporates additional techniques for stability enhancement. In addition to the Crank-Nicholson scheme, Algorithm 2 introduces flux smoothing methods to mitigate potential instabilities, particularly in scenarios involving rapid fluctuations in surface temperature. This approach also considers thermal emission from the surface, factoring in the emissivity of the material. By employing a predictor-corrector scheme [A.2.2], Algorithm 2 further refines temperature predictions, particularly valuable when significant changes in surface temperature are anticipated. Through these enhancements, Algorithm 2 ensures robustness and accuracy in simulating subsurface temperature dynamics.

- Post-simulation Analysis: Load the temperature profile and depth data from the output files. Plot the temperature profiles comparing the numerical solutions obtained from the simulation with analytical solutions for sinusoidal surface temperature oscillations and semi-infinite domain.

This outlines the process to understand temperature variations in the subsurface environment.

4 Results

4.1 Topography generation

Using the parameters for moon, the following topography was observed.

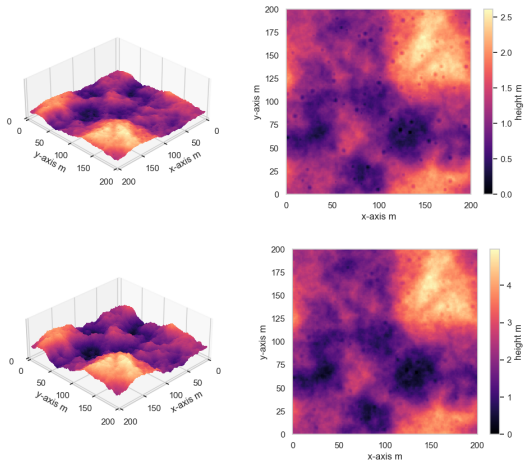

Figure 5: Comparing the effects of fractal amplitude (σ) on roughness [A.2.3] with Random Distribution of craters (a)lower amplitude gain for fractal surface [σ=5]; (b)higher amplitude gain for fractal surface [σ=10]

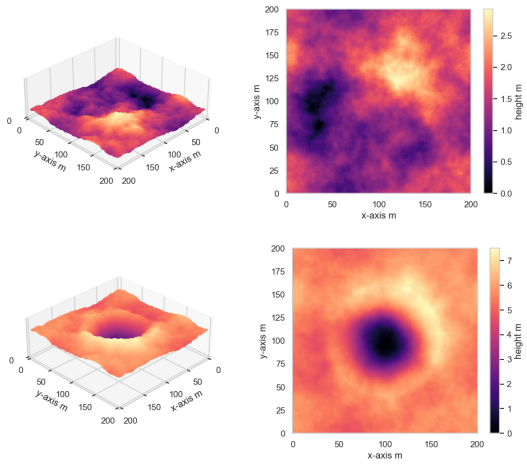

Figure 6: Comparing different distribution of craters with $\sigma = 5$ (a) Plain i.e No craters; (b) Single Crater

The topography for martian surface was also generated besides the lunar topographic map [Lunar ODE] by adjusting the parameters as per the martian parameters [KRC-JMARS]. [Kieffer, 2013]

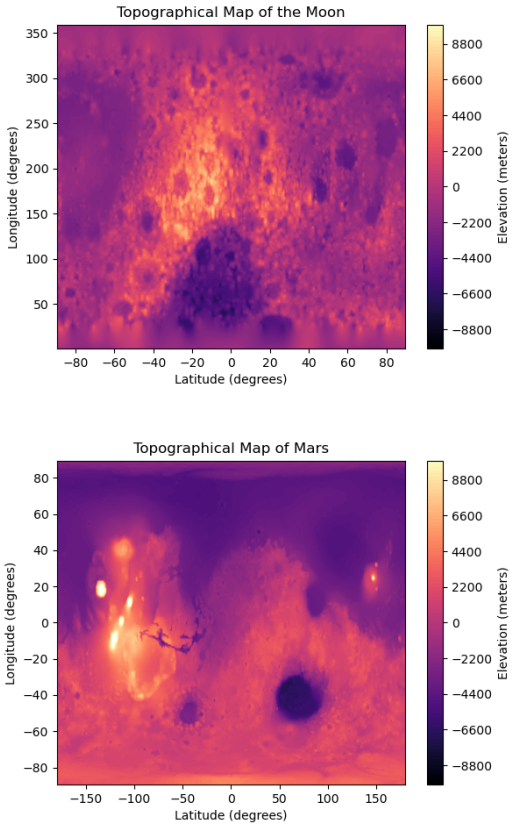

Figure 7: Comparing different planetary surface parameters (a) Lunar surface; (b) Mars surface

4.2 1D Thermal distribution

The parameters used as reference is that of Mars (due to the established KRC model of mars for validating)[Kieffer, 2013]. Using the algorithm 1, The heat diffusion equation under flux conservation was simulated and the solution was obtained as shown by the initial thermal profile for a horizontal unobstructed planar surface [fig. 8] and the evolution of the thermal profile obtained with the solution is shown in fig. 4.2.

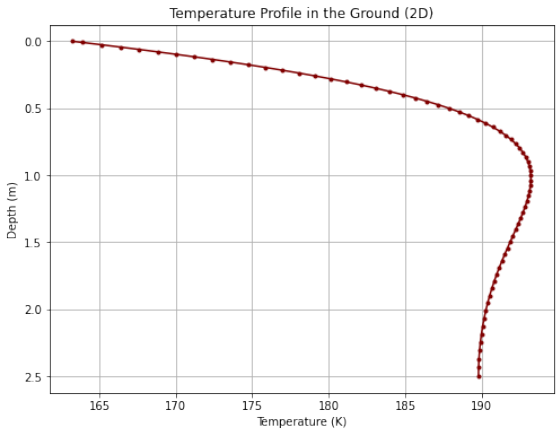

Figure 8: Initial solution for the heat diffusion equation under flux conservation

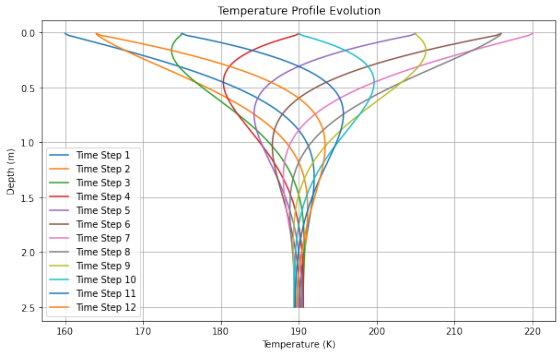

Figure 9: Thermal evolution of the solution under flux conservation with time

The numerical solution for the discretized heat diffusion equation to predict the surface temperature profile under given boundary conditions is compared to the analytical solution for a semi-infinite domain with sinusoidal surface temperature oscillations [A.3.1]. The Superimposed solution [fig. 11] depicts slight deviation as depth increases because the analytical solution is for an infinitely deep domain.

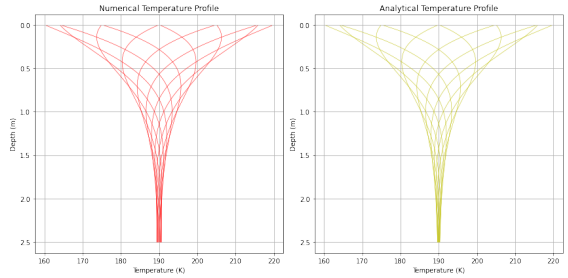

Figure 10: (a) The numerical solution under flux conservation [red] and (b) the analytical solution[yellow]

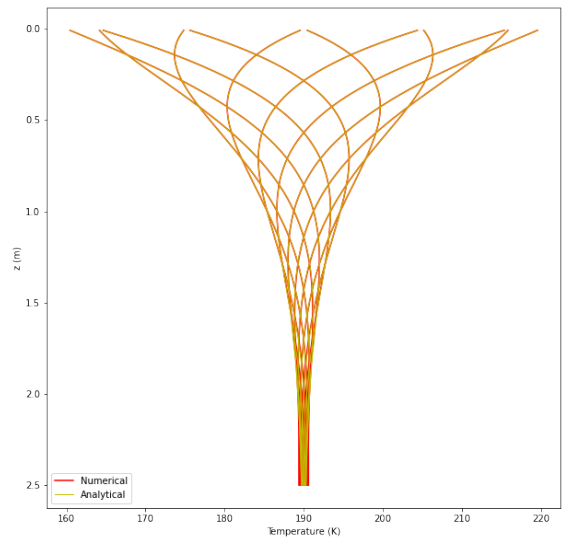

Figure 11: The numerical solution superimposed with the analytical solution.

Similarly, the thermal evolution of the surface considering thermal emission is shown in fig. 12. The comparison against analytical solution is shown in fig. 13

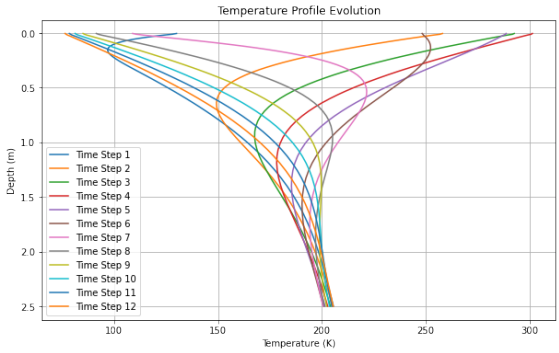

Figure 12: Thermal evolution of the solution with time with changed upper boundary i.e considering thermal emissions

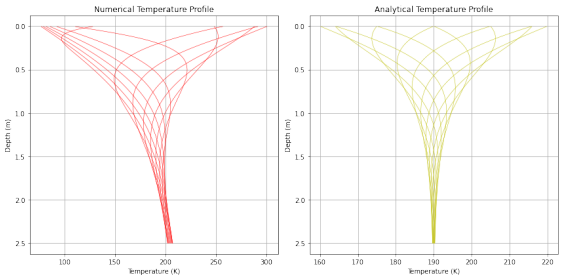

Figure 13: (a) The numerical solution with thermal emissions [red] and (b) the analytical solution[yellow]

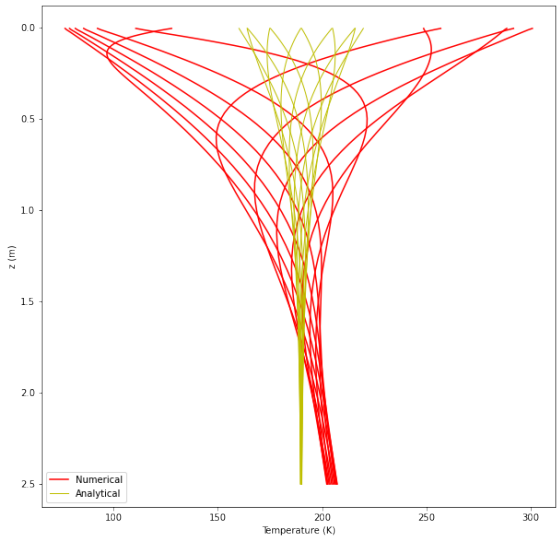

Figure 14: The numerical solution superimposed with the analytical solution.

5 Discussions and Conclusion

In this project, a comprehensive implementation for generating synthetic planetary surfaces with a focus on crater formation and fractal terrain generation is explored. The simulation allows for customization of parameters such as crater distribution, size, and terrain fractality, enabling users to create diverse planetary surface simulations.

With the generated topographic maps for mars and moon, we observe that there are portions of the lunar surface that are depressed (with an altitude below 0 meters) and features that are raised. We also see some wide basins with a fairly consistent altitude across the feature. For the larger topographic features, like the large basins with a fairly consistent altitude across the feature, are the result of the density of the moon's crust while it was forming. The smaller topographic features we see, with a very clearly defined center with a sharp change in altitude associate with it, are likely the result of meteorite impacts is a result of the Moon's lack of an atmosphere.

Meanwhile, Mars has a greater number of large topographical features and very few small topographic features. The primary source of Mars' topographic variability is therefore likely the result of how the crust was formed.

Diving into the temperature distribution, the provided report presents a one-dimensional analysis of heat conduction in a semi-infinite domain with sinusoidal surface temperature oscillations. The numerical and analytical solutions presented in the report offer valuable insights into the thermal behavior of the system with and without taking thermal emissions in account.

It is observed that the average surface temperature increases when the emission of thermal radiation from the surface leads to an increase in the average surface temperature as the system seeks to balance the energy exchange with its surroundings. The emission of thermal radiation also alters the heat distribution within the system, leading to changes in temperature gradients. This can result in regions experiencing higher or lower temperatures than before, thereby increasing the overall temperature variation. The system may respond dynamically to such changes in temperature, leading to non-linear behavior and increased temperature variation over time. This may include phenomena such as thermal inertia, where the system retains heat and releases it gradually, or feedback loops that amplify temperature fluctuations. These variations in temperature may affect the thermal properties of the materials involved, such as conductivity or emissivity, which in turn influence heat transfer dynamics and temperature distribution.

References

Rose, C. (1966). Chapter 2 - the physical environment of agriculture: Part ii. In C. Rose (Ed.), *Agricultural physics* (pp. 30–68). Pergamon. https://doi.org/https://doi.org/10.1016/B978-0-08-011884-0.50007-X

Shepard, M. K., Brackett, R. A., & Arvidson, R. E. (1995). Self-affine (fractal) topography: Surface parameterization and radar scattering. *J. Geophys. Res.*, *100*, 11709–11718.

Helfenstein, P., & Shepard, M. K. (1999). Submillimeter-scale topography of the lunar regolith. *Icarus*, *141*, 107–131.

Kieffer, H. H. (2013). Thermal model for analysis of mars infrared mapping. *Journal of Geophysical Research: Planets*, *118*(3), 451–470. https://doi.org/https://doi.org/10.1029/2012JE004164

Schorghofer, N., & Aharonson, O. (2014). Topographic distortion of impact craters on the moon. *The Astrophysical Journal*, *788*(2), 169. https://doi.org/10.1088/0004-637X/788/2/169

Bandfield, J. L., Hayne, P. O., Williams, J.-P., Greenhagen, B. T., & Paige, D. A. (2015). Lunar surface roughness derived from lro diviner radiometer observations. *Icarus*, *248*, 357–372.

Fractal dimension. (2019). https://en.wikipedia.org/wiki/Fractal_dimension#Fractal_surface_structures

Leahy, F. B. (2021). *Cross-program design specification for natural environments (dsne)* (Other - DSNE Program Document No. SLS-SPEC-159). Marshall Space Flight Center. Redstone Arsenal, Alabama, United States.

Yang, X., Fa, W., Du, J., Xie, M., & Liu, T. (2021). Effect of topographic degradation on small lunar craters: Implications for regolith thickness estimation. *Geophysical Research Letters*, *48*, Article e2021GL095537. https://doi.org/10.1029/2021GL095537

A Appendix

A.1 Crater Generation

A.1.1 Craters density

Based on an analytical model, calculates the number of craters to generate based on the desired crater density and the area of the terrain. The equation used to calculate the number of craters based on crater density is as follows:

$$\text{num\_crater} = \frac{a \times D^b \times \text{area\_t}}{\text{area\_c}}$$

Where num_crater is the estimated number of craters. a and b are coefficients that determine the density of craters. D is the diameter of the craters. area_t is the total area of the terrain grid. area_c is the area of each individual crater. Here:

$$\text{area\_t} = (\text{n} \times \text{res})^2$$

where n is the grid size and res is resolution for generation.

$$\text{area\_c} = \left(\frac{D}{2}\right)^2 \times \pi$$

These calculations provide the areas needed for estimating the number of craters based on the given crater density.

A.1.2 Crater models

Each crater model can defined as:

- Normal Crater: For $0 \leq r \leq 1$, the height of the crater increases exponentially with the distance from the center, reaching a maximum height determined by the parameters a, b, and C. Beyond $r = 1$, the height decreases according to a power-law decay with an exponent α, representing the outer region of the crater.

$$\begin{cases} h = \frac{C \cdot (e^{(b \cdot r)} - e^b}{1 + e^{(a+b \cdot r)}} & \text{for } 0 \leq r \leq 1 \\ h = hr \cdot (r^\alpha - 1) & \text{otherwise} \end{cases}$$

- Central Mound Crater: The crater features a central mound with decreasing height as the distance from the center increases, reaching a minimum height at the rim. The height increases exponentially with the distance from the rim to the outer boundary of the crater.

$$\begin{cases} h = (1 - \frac{r}{rm}) \cdot hm - d0 & \text{for } 0 \leq r \leq rm \\ h = -d0 & \text{for } rm < r \leq rb \\ h = \frac{C \cdot (e^{(b \cdot r0)} - e^b)}{1 + e^{(a+b \cdot r0)}} & \text{for } rb < r \leq 1 \\ h = hr \cdot (r^\alpha - 1) & \text{otherwise} \end{cases}$$

- Flat-Bottomed Crater: The crater has a flat bottom, with a constant depth extending up to a certain distance from the center. Beyond this distance, the height increases exponentially with the distance from the rim to the outer boundary of the crater.

$$\begin{cases} h = -d0 & \text{for } 0 \leq r \leq rb \\ h = \frac{C \cdot (e^{(b \cdot r0)} - e^b)}{1 + e^{(a+b \cdot r0)}} & \text{for } rb < r \leq 1 \\ h = hr \cdot (r^\alpha - 1) & \text{otherwise} \end{cases}$$

- Concentric Crater Model: The crater features multiple concentric rings with varying depths, each described by different polynomial or exponential functions. The height increases exponentially with the distance from the outermost ring to the outer boundary of the crater.

$$\begin{cases} h = C1 \cdot r^2 + C2 \cdot r - d0 & \text{for } 0 \leq r \leq ri \\ h = C3 \cdot (r - ri) + h1 & \text{for } ri < r \leq ro \\ h = \frac{C \cdot (e^{(b \cdot r0)} - e^b)}{1 + e^{(a+b \cdot r0)}} & \text{for } ro < r \leq 1 \\ h = hr \cdot (r^\alpha - 1) & \text{otherwise} \end{cases}$$

A.2 Numerical Methods

A.2.1 Crank-Nicolson Method

The Crank-Nicolson method is a finite difference scheme commonly used to solve partial differential equations, such as the heat diffusion equation. For a one-dimensional heat diffusion equation with time and space discretization, the Crank-Nicolson method can be expressed as follows:

$$\frac{T_i^{n+1} - T_i^n}{\Delta t} = \frac{k_{i+1/2}(T_{i+1}^n - T_i^n) - k_{i-1/2}(T_i^n - T_{i-1}^n)}{\Delta z^2} + \frac{k_{i+1/2}(T_{i+1}^{n+1} - T_i^{n+1}) - k_{i-1/2}(T_i^{n+1} - T_{i-1}^{n+1})}{\Delta z^2}$$

where: - T_i^n represents the temperature at node i and time step n, - Δt is the time step size, - Δz is the spatial grid spacing, - $k_{i+1/2}$ and $k_{i-1/2}$ are the thermal conductivities at the cell interfaces, - T_i^{n+1} is the temperature at node i at the next time step $n + 1$.

A.2.2 Predictor-Corrector Method

The predictor-corrector method is an iterative scheme that improves the accuracy of predictions by refining them through successive correction steps. In the context of numerical simulations for heat diffusion, the

predictor-corrector method can be applied to enhance stability and accuracy. One common form of the predictor-corrector method involves predicting an intermediate solution based on the initial conditions and then correcting this prediction iteratively using a correction term. Mathematically, it can be represented as follows:

- Prediction Step:

$$T_{\text{pred}}^{n+1} = T^n + \Delta t \cdot F(T^n)$$

where T_{pred}^{n+1} represents the predicted temperature at the next time step $n+1$, T^n is the temperature at the current time step n, Δt is the time step size, and $F(T^n)$ is the function representing the heat diffusion process.

- Correction Step:

$$T^{n+1} = T^n + \frac{1}{2} \cdot (\Delta t \cdot F(T^n) + \Delta t \cdot F(T_{\text{pred}}^{n+1}))$$

where T^{n+1} represents the corrected temperature at the next time step $n+1$.

These iterations continue until the solution converges to a desired accuracy, improving the overall stability and accuracy of the numerical simulation.

A.2.3 Fractal Generation

With x_{id} and y_{id} as the coordinates of the grid point.

$$\text{r} = \frac{1}{(x_{id}^2 + y_{id}^2)^{\frac{(r_e+1)}{2}}}$$

Where r is the radius of the point and r_e is the parameter controlling the roughness or smoothness of the surface.
To generate a complex number representing the height value for each grid point with fractional Brownian motion (fBm):

$$z = r \cdot e^{i \cdot \phi}$$

Where: - z is the complex number representing the height value, r is the radius, which determines the amplitude or magnitude of the height value and ϕ is the phase angle, which introduces randomness or spatial variation.

This equation combines the magnitude (amplitude) and phase information into a single complex number, allowing for a compact representation of the height field with both spatial and amplitude characteristics. Then:

$$z' = z \times (\sigma) \times (res)^2 \times n$$

where z' is scaled height values in frequency domains, σ is amplitude for terrain height, *res* is the resolution of the grid that affects the spatial granularity of the generated terrain and n is grid size to determine the overall extent of the generated terrain. The hieght values in frequency domains is then converted to spatia domain for visualisation:

$$z(x, y) = ifft2(Z(u, v))$$

A.3 Thermal modelling: KRC

The KRC (K for conductivity, R for density, C for specific heat) model stands as a cornerstone in planetary science research, particularly in the study of Martian surface temperatures and the support of planetary missions. Developed using explicit forward finite differences and implemented in FORTRAN with supplementary utility C routines, this numerical thermal simulation tool embodies fundamental physical parameters to understand the thermal behavior of planetary surfaces. This parameter is thermal inertia that dictates the surface's resistance to temperature changes, shedding light on its composition and thermal dynamics. The expression for thermal inertia (I) in the KRC model is given by:

$$I = \sqrt{k \cdot \rho \cdot C}$$

where k is the thermal conductivity, ρ is the bulk density, and C is the specific heat capacity.

A.3.1 Analytical solution for heat diffusion

The analytical solution for a semi-infinite domain with sinusoidal surface temperature oscillations can be described by the one-dimensional heat conduction equation. Assuming a semi-infinite domain, where the depth is much larger than the characteristic length scale of temperature variations, and considering sinusoidal surface temperature oscillations, the equation can be written as:

$$T(z, t) = T_m + A \exp\left(-\frac{z}{\delta}\right) \sin\left(\frac{z}{\delta} - \omega t\right)$$

Where $T(z,t)$ is the temperature at depth z and time t, T_m is the mean temperature at depth z, A is the amplitude of temperature oscillations and ω is the angular frequency of the surface temperature oscillations as $\omega = 2\pi/P$.

The thermal skin depth δ is given by:

$$\delta = \sqrt{\frac{\alpha \cdot t}{\pi}} = \frac{\Gamma}{\rho c}\sqrt{\frac{P}{\pi}}$$

where α is the thermal diffusivity of the material and P is the period.